www.cad-journal.net
Computer-Aided Design AND APPLICATIONS

Design of a Novel Underactuated Robotic Hand with Rigid-flexible Variable Fingers and a Deployable Palm

Ruiqin Wang[1], Jiaqi Gu[1], Jian S. Dai[2] and Shijie Dai[1]

[1]Hebei University of Technology, China, wruiqin@foxmail.com, gujiaqi5632@foxmail.com, dsj@hebut.edu.cn
[2]Southern University of Science and Technology, China, jian.dai@kcl.ac.uk

Corresponding author: Ruiqin Wang, wruiqin@foxmail.com

Abstract. Aiming to improve the versatility and gripping stability, this paper proposed a novel underactuated robotic hand with rigid-flexible variable fingers and a deployable palm. The special structure of torsion springs and cables composed in the fingers can achieve flexible contact and adaptive gripping. By configuring reset torsion springs with different stiffness, fingers can achieve different motion trajectories. The deployable palm can simultaneously achieve the rotation and distance adjustment of finger bases. The palm improves the range and stability of gripping objects. The robotic hand can achieve different gripping modes, such as enveloping gripping and parallel gripping of small objects. Afterwards, the parameters of the torsion spring are determined based on the selected finger motion trajectory. Finally, the motion and feasibility of the robotic hand are simulated and verified in Adams.

Keywords: Robotic Hands, Underactuated Mechanism, Mechanism Design, Self-Adaptive.
DOI: https://doi.org/10.14733/cadaps.2026.249-258

1 INTRODUCTION

As an important end effector, robotic hands have always been a focus of research for researchers. According to the relationship between the number of active components and degrees of freedom in the system, robotic hands can be divided into two categories: fully actuated robotic hands and underactuated robotic hands. The fully driven robotic hand has high flexibility and powerful grasping function, but it has many sensors, a relatively large volume, and complex control. In comparison, underactuated robotic hands are more reliable, cost-effective, and easier to control due to their simplified structure of driving and transmission. Therefore, underactuated robotic hands have become one of the main research directions for robotic hands.

Adaptive fingers, through the design of spring constraints or mechanism triggers, stop the motion of one finger bone when it touches an object, and then the next finger bone begins to move, changing the number of active components in the system, thus achieving a step-by-step

motion of each finger bone until the last finger bone contacts the object, completing the enveloping grip of objects of different shapes. However, due to the non-linear motion trajectory of the fingertips in grasping or pinching mode, it is difficult for the fingers to grasp small or thin objects. To address this issue, LUO et al. [7] proposed a novel linear mechanism and designed a two-finger bone robot finger VGS with a hybrid grasping mode. Li et al. [6] designed an underactuated robotic hand that combines linear pinching and adaptive grasping modes, and analyzed its motion trajectory and contact force. However, this type of finger can only convert from linear mode to envelope grasping mode when it is driven by external force, which inevitably inherits the shortcomings of adaptive fingers. Specifically, when the finger bones come into contact with an object, there is inevitably a contact force between the finger bones and the grasped object, which may cause damage to some fragile or soft objects during the adaptive finger grasping process, or affect the grasping effect [4]. Some researchers have proposed coupling adaptive fingers to reduce the contact force generated by fingers when adapting to objects, and to some extent prevent objects from escaping and improve grasping effectiveness by simultaneously driving several joint motions through a driver [3],[11],[12]. Some researchers have also proposed variable stiffness structures for grasping soft objects. Fu et al. [2] proposed a novel variable stiffness gripper (VSG), which is designed based on a parallel guide beam structure. A slider is inserted from one end to achieve stiffness changes by changing the length of the parallel beams involved in the system.

The study of palm structure has further developed the performance of robotic hands. For three-finger robotic hands, some robotic hands use a rotating mechanism to change the direction of the finger surface, thereby improving the adaptability of the gripper and enabling it to grasp objects of various geometric shapes [8-10]. In addition, there are also some robotic hands that can change the distance between finger bases by moving them on a track, thereby improving the gripping space of the robotic hand and enhancing the effectiveness of the robotic hand's grip [1],[5]. However, few robotic hands can simultaneously possess both of the above properties.

In practical applications of underactuated robotic hands, especially when performing complex tasks in unstructured environments such as collecting planetary ores of different sizes, picking fruits and vegetables of various shapes, and grasping a wide variety of household items, the performance of robotic hands often directly determines the success rate of grasping tasks.

This article proposes a robotic hand with multiple functions. Its fingers can achieve coupling adaptation, reducing the contact force generated before the fingers envelop the object. And analyzing its motion trajectory, it was found that the finger's motion trajectory can be changed by changing the stiffness of the reset torsion spring, which may enable the object to be enveloped before applying a contact force when grasping a certain shape. The robotic hand palm has a rotating mechanism and a deployable mechanism, which can reconstruct the appropriate finger surface angle and finger base distance when grasping objects of different sizes and shapes, improving the stability of grasping. In addition, the joint use of deployable mechanisms and finger bending can enable the robotic hand to grip with a certain stiffness. The robotic hand proposed in this article can work in multiple modes to complete different grasping tasks.

2 STRUCTURE DESIGN

2.1 Overall Design of the Robotic Hand

For underactuated multi-finger robotic hands, the number of fingers has a significant impact on grasping stability. In the design process of a robotic hand, the complexity of its structure increases with the number of fingers, and the number of driving devices also increases accordingly, leading to difficulties in controlling the gripper. The three fingers basically meet the grasping requirements of the robotic hand for objects, so the robotic hand proposed in this article has three fingers, and the overall structure is shown in Figure 1. The robotic hand is mainly composed of 3 fingers, a palm, a frame, and a motor, with a total of 12 degrees of freedom. The rotational degrees of

freedom of finger 1 and finger 2 in the horizontal direction are directly controlled by the motor, making it easy for the fingers to reorient and adhere to objects. In addition, their bending degrees of freedom are controlled by one motor, and the bending degrees of freedom of finger three are controlled by another motor. The vertical motion freedom of the moving platform of the palm is controlled by a linear motor, combined with a deployable mechanism, which can change the finger spacing and adapt to objects of different sizes.

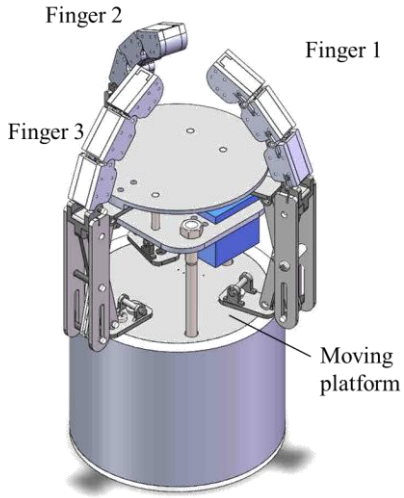

Figure 1: Overall structure of the robotic hand.

2.2 Finger Structure

Based on the underactuated principle, this paper designs a new adaptive finger structure. The 3D model of the finger is shown in Figure 2. Fingers are composed of three finger phalanxes, three pulley groups, torsion springs, and reset torsion springs. Each joint's torsion spring is connected to the corresponding pulley and finger phalanx. Specifically, one end of the torsion spring at the metacarpophalangeal (MCP) joint is fixed to the pulley, and the other end is connected to the first finger phalanx. Adjacent pulleys are connected by cables. In addition, there is a reset torsion spring on the side of the finger to restore its initial position. When the cable is pulled by the motor, the motion trajectory of the fingers will exhibit different behaviors due to the difference in stiffness between the torsion spring and the reset torsion spring.

When the stiffness of the reset torsion spring is negligible relative to the torsion spring, the motion trajectory of the fingers presents a situation where the three phalanges rotate as a whole around the MCP joint, as shown in Figure 3. The specific situation is explained as follows:

The motor applies torque to the pulley at the MCP joint by pulling the cable, causing it to rotate relative to the base of the finger. Due to the torsion spring being fixed between the pulley and the phalanx, the pulley will transmit torque to the phalanx through the torsion spring, causing it to rotate. On the other hand, the proximal interphalangeal (PIP) pulley connected to the MCP joint pulley through a cable does not rotate relative to the first phalanx after following the rotation of the first phalanx, which means that the second phalanx does not rotate relative to the first phalanx, and the third phalanx does the same, so that the three phalanxs rotate around the MCP joint.

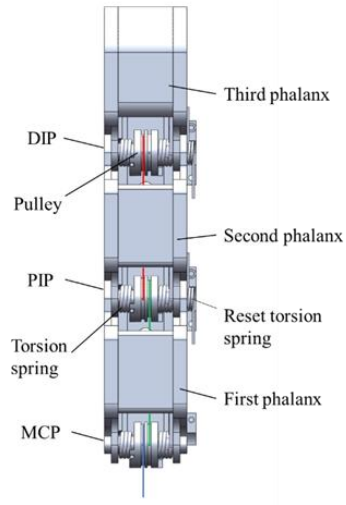

Figure 2: Finger structure.

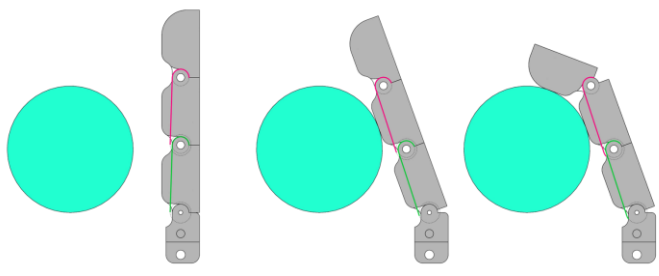

Figure 3: The first motion: rotate around the MCP joint.

When the stiffness of the reset torsion spring affects the torsion spring, the motion trajectory of the fingers presents as three finger phalanxes rotating simultaneously. The specific situation is explained as follows:

The motor pulls the cable, and after the first phalanx is rotated by the torsion spring, the reset torsion spring at the base of the phalanx and finger will deform, causing greater resistance torque to the finger, thus requiring the torsion spring to increase the torsion angle. When the MCP pulley experiences an increase in the torsion angle of the torsion spring during rotation, the pulley will pull the PIP pulley through a cable, causing it to rotate a certain angle relative to the first phalanx, thus repeating the motion of the MCP joint at the PIP joint, that is, the first phalanx rotates relative to the base of the finger, and the second phalanx rotates relative to the first phalanx. Similarly, the third phalanx also has relative rotation, causing all three phalanges of the finger to bend simultaneously.

For the above two motion states, when the finger rotates to contact the object, if the target object first comes into contact with the first or second phalanx, the drive of the motor will cause the pulley to continue rotating with the increase of the twist angle, thereby transmitting the torque to the next stage through the cable, and ultimately causing the unsecured phalanx to continue

rotating until it contacts the object. If the object first comes into contact with the third phalanx, the contact force can be increased directly by increasing the torsion angle.

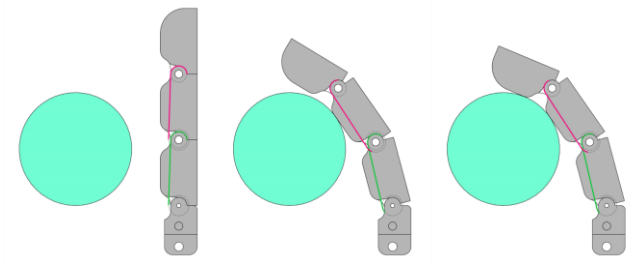

Figure 4: The second motion: three joints rotate simultaneously.

In addition, for the second motion, when the finger bone rotates, the stiffness of the reset torsion spring is different, resulting in different resistance moments, which affect the increased torsion angle of the torsion spring and thus affect the angle of rotation of the next finger bone. This indicates that different stiffness of the reset torsion spring can lead to differences in the proportion of the rotation angles of the three phalanges. In this regard, when grasping an object, we can find the proportion of the rotation angles of the three phalanges at full envelope based on its geometric shape, and make reasonable changes to the stiffness of the reset torsion spring. Therefore, under the drive of a certain torque, the fingers will generate a contact force after fully enveloping the object, thereby further reducing the damage caused to the object by the fingers during the adaptive process.

2.3 Palm Structure

The palm structure proposed in this paper is shown in Figure 5, which mainly includes a moving platform, a rotating mechanism, a deployable mechanism, a frame, a servo motor, and a linear motor. The fingers connected to the rotating mechanism can be directly driven by a motor to change the orientation of the finger contact surface, thereby better fitting the object. The moving platform is driven by a linear motor, which changes the degree of expansion and contraction of the extended structure through the distance moved by the moving platform, thereby changing the position of the fingers. The reason for choosing this deployable mechanism is that it allows the robotic hand to have a smaller initial volume.

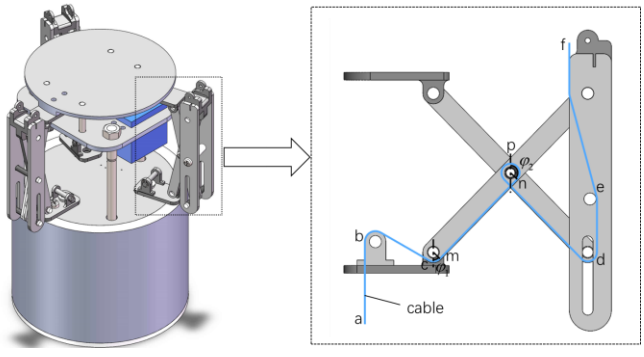

Figure 5: Palm structure.

In order to ensure that the rotation of the rotating mechanism, the motion of the deployable mechanism, and the bending of the fingers do not interfere with each other, it is necessary to arrange the cable reasonably. The arrangement of cables is shown in Figure 5. Firstly, the cable needs to pass through the rotation center axis of the rotating mechanism. Secondly, during the motion of the deployable mechanism, the length of the cable needs to remain constant, that is, the distance from point a to point f needs to be kept constant, otherwise the fingers will bend during the deployable process.

Due to the fact that during the motion of the moving platform, the position of point b relative to point c and point e relative to point f remains relatively unchanged, and the change distance between points a and b is the same as the change size between points d and e. Therefore, it is only necessary to ensure that the length of the cable from point c to point d remains unchanged. According to Figure 5, the length of the cable in the CD segment can be calculated as:

$$l_{CD} = 2l_{CP} = 2\mathrm{R}_1\varphi_1 + 2\mathrm{L} + 2\mathrm{R}_2\varphi_2 \tag{2.1}$$

where R_1 and R_2 respectively represent the radius of the pulley at c and p; L represents the distance between the centers of the pulleys at c and p; According to geometric relationships, $\varphi_1 + \varphi_2 = \pi$. Therefore,when $\mathrm{R}_1 = \mathrm{R}_2$ the length of the CD segment cable is a constant value.

3 PARAMETER DETERMINATION

In this section, we will analyze the second type of motion trajectory and solve the relationship between the ratio of the rotation angles of the three joints and the torsion spring, in order to determine the torsion spring parameters based on different trajectories.

Firstly, clarify that the angle of pulley rotation is divided into the torsion angle of the torsion spring and the rotation angle of the finger phalanx:

$$\theta_{pi} = \theta_{si} + \theta_{ri} \tag{3.1}$$

where θ_{pi} represents the angle of rotation of pulley i, θ_{si} represents the torsion angle of torsion spring i, and θ_{ri} represents the angle of bending of the phalanx i. The relationship between the rotation angles of adjacent pulleys is:

$$\theta_{p,i+1} = r_i\theta_{si} \tag{3.2}$$

where r_i represents the radius ratio of pulley i to pulley $i+1$. Here, we introduce parameters: $n_{i,i+1} = \dfrac{\theta_{si}}{\theta_{s,i+1}}$, $ra_i = \dfrac{\theta_{ri}}{\theta_{si}}$,and according to equations (3.1) and (3.2), we can conclude that $n_{i,i+1} = \dfrac{ra_{i+1}+1}{r_i}$. Thus, the ratio of the rotation angle of the finger before contacting the object is DIP: PIP: MCP= $ra_3 : \dfrac{ra_2\ ra_3+1}{r_2} : \dfrac{ra_1\ ra_2+1\quad ra_3+1}{r_1 r_2}$. Thus, ra can be selected according to the required ratio, and $n_{i,i+1}$ can be calculated based on the already selected radius ratio.

Afterwards, based on the torque balance, a force analysis of the fingers can be conducted, and it can be concluded that:

$$\mathrm{T}_i = \begin{cases} \mathrm{T}_{ci} + \mathrm{T}_{si} & i = 1,2 \\ \mathrm{T}_{si} & i = 3 \end{cases} \tag{3.3}$$

$$\mathrm{T}_i = \mathrm{T}_{Mi} \tag{3.4}$$

where T_{i} represents the driving torque generated by the cable on pulley i, T_{ci} represents the torque generated by pulley $i+1$ on pulley i, T_{si} represents the torque generated by the torsion spring i on pulley i, and T_{Mi} represents the torque generated by the reset torsion spring.

By connecting the above equations, the expression for the stiffness of the reset torsion spring can be obtained:

$$\begin{cases} k_{33} = k_3 ra_3 \\ k_{22} = \dfrac{k_2 n_{23} + k_3 r_2}{n_{23} ra_2} \\ k_{11} = \dfrac{k_1 n_{12} n_{23} + k_2 n_{23} r_1 + k_3 r_1 r_2}{n_{12} n_{23} ra_1} \end{cases} \tag{3.5}$$

where k_i represents the stiffness of the torsion spring i, and k_{ii} represents the stiffness of the reset torsion spring i. Considering that the torsion spring has a maximum rotation angle, if the rotation angle of the torsion spring exceeds the maximum rotation angle, it will cause the spring to fail and the material to undergo plastic deformation, making it impossible to restore its original state. The speed at which the torsion angle of the torsion spring increases before and after the finger comes into contact with the object is not the same, and the torsion angle ratios are DIP: PIP: MCP= $1:\ n_{23} : n_{12} n_{23}$,DIP: PIP: MCP= $r_1 r_2 : r_1 : 1$. In order for the torsion spring to transmit more torque, $n_{i,i+1}$ should be greater than 1.

In this article, the finger parameters we selected are ($k_1, k_2, k_3, r_1, r_2, ra_3$)=($0.56, 0.56, 1.3, 2.5, 2.5, 2$), Using DIP:PIP:MCP=1:1.2:1.44 as the objective, solve for $ra_1 = ra_2 = 2$, $n_{12} = n_{23} = 1.2$,The stiffness of the reset torsion spring is $k_{11} = 3.68, k_{22} = 1.63, k_{33} = 0.65$.

4 SIMULATION

In this section, the influence of torsion springs on finger motion trajectories and the influence of deployable mechanism motion on finger bending motion will be verified in Adams.

Firstly, import the finger model into Adams, set constraints, contacts, and other aspects, and establish the cable through the software's built-in cable module. Set the torsion spring force, but do not set the reset torsion spring. Apply a torque under the finger and simulate it in a short period of time. The simulation results of finger rotation angle are shown in Figure 6, where only the MCP joint rotates.

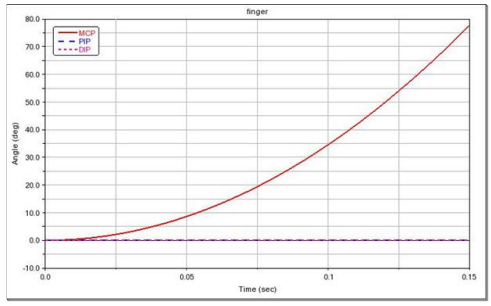

Figure 6: Rotation angle of finger in the first motion.

Afterwards, set the reset torsion spring, apply a constant torque under the finger, and simulate it. The simulation results of the torsion spring and finger rotation angle are shown in Figures 7 and 8. The results showed that during the simulation, MCP, PIP, and DIP joints all underwent bending motions, and the ratio of their rotation angles was 48.91°: 40.68°: 33.65°, which was similar to the expected results.

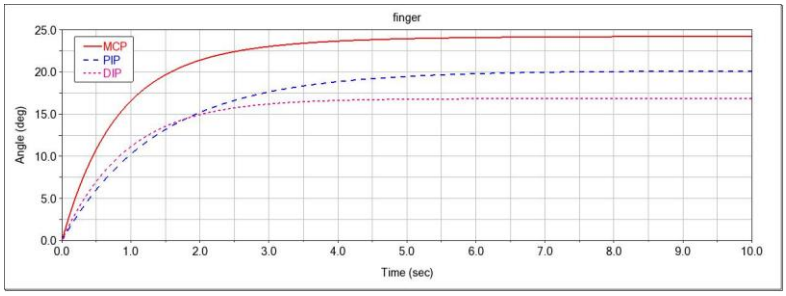

Figure 7: The torsion angle of a torsion spring.

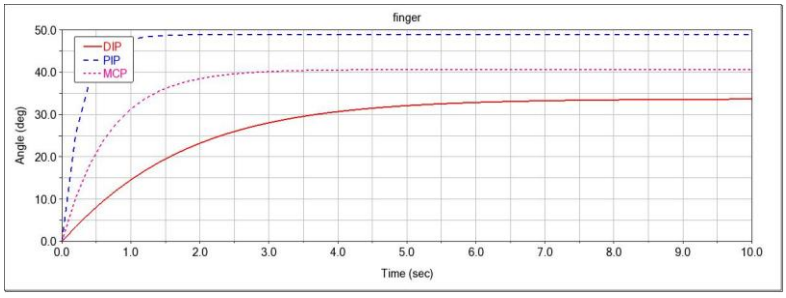

Figure 8: The rotation angle of the finger.

Next, the influence of the deployable mechanism on finger bending motion will be verified in Adams. Firstly, import the robotic hand model into Adams and complete the establishment of constraints, contacts, and cables. The model is shown in Figure 9. Afterwards, create a linear drive for the moving platform and apply a torque expression of step (time, 0, 10, 4, 72) to the finger cable for simulation. After the simulation is completed, save the results and cancel the linear drive. Fix the moving platform to the ground and perform the simulation again. The bending results of the fingers in the two simulations are shown in Figure 10. The bending angle using the deployable mechanism is similar to the bending angle fixed between the moving platform and the ground. This indicates that the deployable motion of the robotic hand is independent of the bending motion of the fingers, and the robotic hand can freely change the distance between the fingers to better grasp objects of different sizes. Alternatively, bending the fingers to a certain stiffness and moving them to the side of a small object through deployable motion for gripping.

5 CONCLUSIONS

A robotic hand structure with multiple functions has been proposed. The fingers use a special structure composed of torsion springs and cables. Due to the variable torsion angle of the torsion spring, fingers can achieve flexible contact and adaptive grasping. The palm is composed of a rotating structure and a deployable mechanism, which can simultaneously achieve rotation and distance adjustment of the finger base. Therefore, the robotic hand can reconstruct the palm

according to different grasping objects, achieving enveloping grasping or parallel pinching. Afterwards, the influence of the stiffness of the torsion spring on the trajectory of finger movement was studied, and the relationship between the trajectory and the stiffness of the reset torsion spring was obtained. And take a motion trajectory as an example to calculate it.

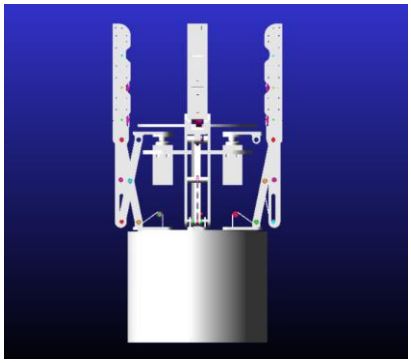

Figure 9: Adams model.

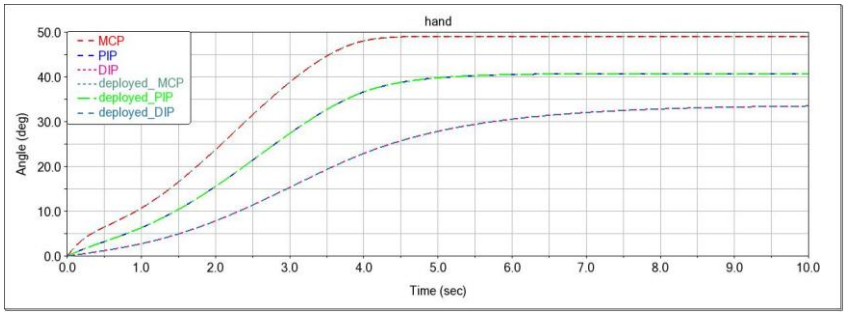

Figure 10: Rotation angle of finger with and without deployment mechanism.

Finally, the motion and feasibility of the robotic hand were simulated and validated in Adams. In the simulation of finger motion, the rotation of the finger around the MCP and the simultaneous rotation of the three joints of the finger were achieved according to different settings of the torsion spring. And the rotation angles of the coupled motion are 48.91°, 40.68°, and 33.65°, respectively, which are consistent with our theoretical calculations. The simulation results of the deployable mechanism and cable arrangement indicate that the reconstruction of the palm does not affect the motion of the fingers. Thus, improving the adaptability of the robotic hand to different objects. Due to the current research stage, the robotic hand proposed in this article has not yet been physically prototyped and experimentally validated, and its actual performance needs further confirmation.

Ruiqin Wang, https://orcid.org/0000-0002-3087-3203
Jian S. Dai, https://orcid.org/0000-0002-9729-1662
Shijie Dai, https://orcid.org/0000-0002-9082-9984

REFERENCES

[1] Elangovan, N.; Gerez, L.; Gao, G.; Liarokapis M.: A multi-modal robotic gripper with a reconfigurable base: Improving dexterous manipulation without compromising grasping

efficiency, 2021 IEEE/RSJ International Conference on Intelligent Robots and Systems (IROS), IEEE, 2021, 6124-6130. https://doi.org/10.1109/IROS51168.2021.9636392

[2] Fu, J.; Yu, Z.; Guo, Q.: A variable stiffness robotic gripper based on parallel beam with vision-based force sensing for flexible grasping, Robotica, 2023, 1-19. https://doi.org/10.1017/S026357472300156X

[3] Hirano, D.; Nagaoka, K.; Yoshida, K.: Design of underactuated hand for caging-based grasping of free-flying object, Proceedings of the 2013 IEEE/SICE International Symposium on System Integration, Kobe, Japan, IEEE, 2013, 436-442. https://doi.org/10.1109/SII.2013.6776675

[4] Higashimori, M.; Kaneko, M.; Ishikawa, M.: Dynamic preshaping for a robot driven by a single wire, 2003 IEEE International Conference on Robotics and Automation (Cat. No. 03CH37422), IEEE, 2003, 1, 1115-1120. https://doi.org/10.1109/ROBOT.2003.1241742

[5] Jiang, Q.; Xu, F.: Design and motion analysis of adjustable pneumatic soft manipulator for grasping object, IEEE Access, 2020, 8, 191920-191929. https://doi.org/10.1109/ACCESS.2020.3032842

[6] LI, X.P.; GUO, J.Q.; SUN, W.Q.: Design and contact force analysis of under-actuated manipulator with hybrid working mode, Journal of Mechanical Engineering, 2021, 57(1), 8-18.https://doi.org/10.3901/JME.2021.01.008

[7] LUO, C.; ZHANG, W.Z.: VGS hand: A novel hybrid grasping modes robot hand with variable geometrical structure, Applied Sciences, 2019, 9(8), 1-14. https://doi.org/10.3390/app9081566.

[8] Lu, Q.; Baron, N.; Clark, A.B.; Rojas, N.: Systematic object-invariant in-hand manipulation via reconfigurable underactuation: Introducing the RUTH gripper, The International Journal of Robotics Research, 2021, 40(12-14), 1402-1418. https://doi.org/10.1177/02783649211048929

[9] Mathew, A.T.; Hussain, I.; Stefanini, C.; Benhmida, I.M.; Renda, F.: ReSoft Gripper: A reconfigurable soft gripper with monolithic fingers and differential mechanism for versatile and delicate grasping, 2021 IEEE 4th International Conference on Soft Robotics (RoboSoft). IEEE, 2021, 372-378. https://doi.org/10.1109/RoboSoft51838.2021.9479341

[10] Meng, H.; Yang, K.; Zhou, L.; Shi, Y.X.; Cai, S.B.; Bao, G.J.: Optimal Design of Linkage-Driven Underactuated Hand for Precise Pinching and Powerful Grasping, IEEE Robotics and Automation Letters, 2024, 9(4), 3475-3482. https://doi.org/10.1109/LRA.2024.3369941

[11] Sun, J.; Zhang, W.: A novel coupled and self-adaptive under-actuated multi-fingered hand with gear–rack–slider mechanism, Journal of Manufacturing Systems, 2012, 31(1), 42-49. https://doi.org/10.1016/j.jmsy.2011.09.001

[12] Yoon, D.; Choi, Y.: Underactuated finger mechanism using contractible slider-cranks and stackable four-bar linkages, IEEE/ASME Transactions on Mechatronics, 2017, 22(5), 2046-2057. https://doi.org/10.1109/TMECH.2017.2723718